

O₂ Adsorption on Defective Penta-Graphene Lattices: A DFT Study

Kleuton A. Lopes Lima^a, Marcelo L. Pereira Júnior^a, Fábio F. Monteiro^a, Luiz F. Roncaratti Júnior^a and Luiz A. Ribeiro Júnior^{a,*}

^aInstitute of Physics, University of Brasília, 70910-900, Brasília, Brazil

ARTICLE INFO

Keywords:

Oxygen Adsorption
Penta-Graphene
Sensors
DFT
Improved Lennard-Jones

ABSTRACT

Penta-Graphene (PG) was theoretically proposed as a new carbon allotrope with a 2D structure. PG has revealed interesting gas sensing properties. Here, the structural and electronic properties of defective PG lattices interacting with an oxygen molecule were theoretically studied by employing density functional theory calculations. Results show that PG lattices with a sp^3 -like single-atom vacancy presented higher adsorption energy than the sp^2 -like one. Remarkably, PG lattices with a sp^3 -like defect presented a clear degree of selectivity for the molecule orientation by changing their bandgap configurations. Importantly, the adsorption energies were obtained using the improved Lennard-Jones (ILJ) potential.

1. Introduction

In the last two decades, the need for environmental, industrial, and biological monitoring of O₂ concentration has stimulated the growing interest in developing new oxygen sensor technologies [1–3]. Carbon-based 3D and 2D nanomaterials are known as suitable sensors of small molecules such as O₂, CO, NO, and NO₂ with the potential of monitoring low concentrations of these gases, presenting optimal response times [4–10]. Particularly, 2D structures of these nanomaterials have been both experimentally and theoretically studied regarding their potential of acting as gas sensors, mostly due to their large surface area and high carrier mobility [11–13]. In this sense, it was reported recently that the electronic properties of 2D nanomaterials, such as graphene and MoS₂, are altered upon adsorption of small molecules [14, 15].

Pristine graphene presents a stable sp^2 -like hybridization of carbon bonds and null bandgap [16–18]. These features make it inefficient for gas adsorption and, therefore, not suitable for developing gas sensor devices. On the other hand, Penta-Graphene (PG) — a new 2D carbon allotrope with a Cairo tessellation based lattice (pentagonal arrangement of atoms) [19, 20] — was theoretically proposed as a structure that contains both sp^3 -like and sp^2 -like hybridizations of carbon bonds, which are more interesting when it comes to open new channels for the gas adsorption mechanism [21, 22]. Due to the tetrahedral character of the sp^3 -like hybridization, the PG surface is not precisely flat, which suggests the existence of regions with a higher chance for the adsorption of molecules. This particular feature also broadens the options to use PG as an active layer in novel sensor prototypes [19]. Although PG has shown promising

*Corresponding author

✉ ribeirojr@unb.br (L.A.R. Júnior)

ORCID(s):

trends to develop gas sensor applications [23], due to its unavailability of synthesis, investigations in this direction are still scarce.

Some theoretical contributions in the literature, mostly based on the density functional theory (DFT) calculations, have investigated the adsorption mechanism of small molecules in PG [23, 24, 24–30]. Generally, the results have revealed the existence of substantial adsorption energies for the complex molecule/PG with moderate charge transfer for small molecules such as H₂O, H₂S, NH₃, SO₂, and NO [25]. When it comes to the adsorption mechanism of oxygen molecules on PG lattices, studies in the literature are very few [26]. It is well known that the presence of lattice defects is inevitable during the manufacturing process of nanomaterials [31–33]. In this sense, investigations that take into account the impact of single-atom vacancies on the interaction between small molecules and PG membranes can contribute to gain a broader understanding of the adsorption mechanism in systems with carbon-based active layers.

Herein, we employed DFT calculations to numerically study the effect of O₂ adsorption on the electronic and structural properties of PG lattices endowed of single-atom vacancies. Remarkably, our results point to the possibility of O₂ adsorption on PG at room temperature with reasonable adsorption energy, low recovering time, and a good degree of selectivity. The calculations performed here suggest that PG can be a promising candidate for the production of O₂ sensors and open a channel for the understanding of the adsorption mechanism of small molecules in carbon-based lattices.

2. Methodology

The structural and electronic properties of PG/O₂ complexes were studied using the DMol³ module as implemented in Biovia Materials Studio software [34–36]. In all calculations, the Local Density Approximation (LDA) is considered employing the Perdew-Wang (PWC) functional with unrestricted spin (DNP), and a numerical basis set of atomic orbitals with polarized functions [37, 38]. The BSSE correction is used through the counterpoise method, and the nuclei-valence electron interactions are represented by the inclusion of semi-core DFT pseudopotentials [39]. The K points in the Brillouin zone are considered within a $14 \times 14 \times 1$ Monkhorst-Pack mesh [40]. Ground state structures for the PG lattices, as presented in Figure 1, are obtained by defining the following tolerances: 1×10^{-5} for the self-consistent field, 0.002 Ha/Å for maximum force, and 0.005 Å for maximum displacement. A 3×3 supercell with a vacuum space of 30 Å is used to model the interacting PG/O₂ complexes. It is worthwhile to stress that this set of parameters was successfully used in other theoretical studies, where the adsorption of small molecules on the surface of nanostructures was also investigated [41–44].

In Figure 1, the PG lattices contain sp^3 -hybridized carbon atoms (black spheres) and sp^2 -hybridized carbon atoms (gray spheres). Figure 1(a) presents the ground state structure for a non-defective lattice (PG). Figures 1(b) and 1(c) depict the ground state structures for PG lattices with a monovacancy defect at sp^3 -hybridized (PG@A) and sp^2 -

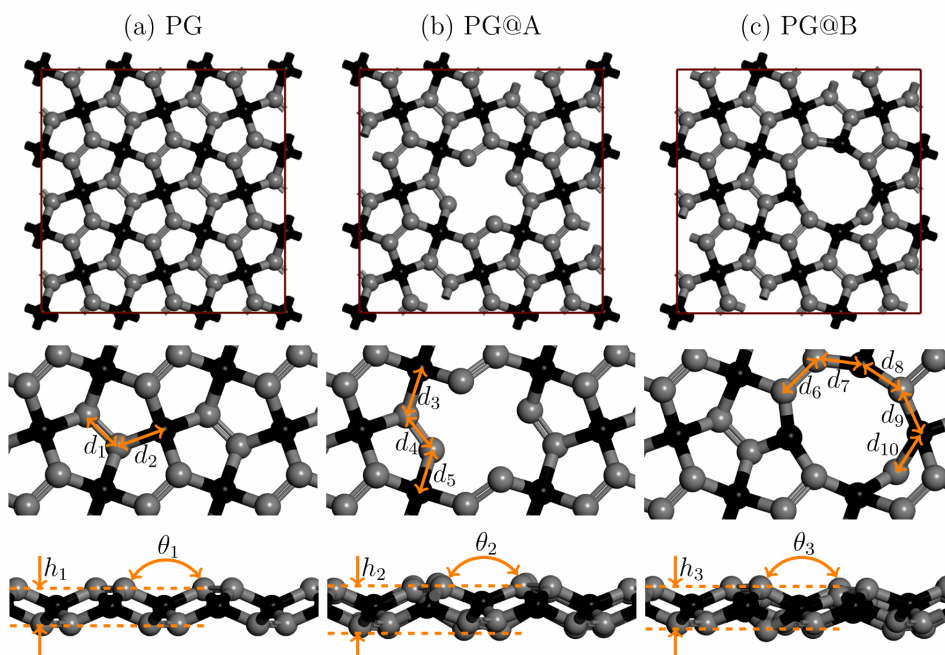


Figure 1: Top panels: Schematic representation for the ground state configurations of (a) non-defective PG, (b) a PG lattice with monovacancy defect at a sp^3 -hybridized carbon atom, and (c) a PG lattice with monovacancy defect at a sp^2 -hybridized carbon atom. Middle panels: enlarged regions to highlight the lattice defects. Bottom panels: side view of the PG lattices. In the color scheme, the sp^3 -hybridized carbon atoms are the black spheres and sp^2 -hybridized carbon atoms are the gray ones.

hybridized carbon (PG@B) atoms, respectively. It is worthwhile to stress that these structures were studied very recently [27]. The structural parameters obtained here (highlighted in Figure 1) are d (in-plane C–C distance), h (out-of-plane C–C distance), and θ (planarity degree). Their values are: $d_1 = 1.34 \text{ \AA}$, $d_2 = 1.54 \text{ \AA}$, $d_3 = 1.55 \text{ \AA}$, $d_4 = 1.33 \text{ \AA}$, $d_5 = 1.50 \text{ \AA}$, $d_6 = 1.37 \text{ \AA}$, $d_7 = 1.41 \text{ \AA}$, $d_8 = 1.45 \text{ \AA}$, $d_9 = 1.51 \text{ \AA}$, $d_{10} = 1.51 \text{ \AA}$, $h_1 = 0.039 \text{ \AA}$, $h_2 = 0.050 \text{ \AA}$, $h_3 = 0.047 \text{ \AA}$, $\theta_1 = 135.01^\circ$, $\theta_2 = 139.21^\circ$, and $\theta_3 = 137.63^\circ$. Importantly, these values are in good agreement with the ones reported in other theoretical studies in literature [23, 27].

In our computational approach, the O₂ molecule is positioned parallel (O₂-H) or perpendicular (O₂-V) to the PG plane, at an initial distance of 7.0 \AA (see Figure 2). The adsorption mechanism for these PG/O₂ complexes was investigated considering six cases, where the O₂ molecule approaches the PG, PG@A, and PG@B surfaces, forming the following complexes: PG/O₂-H, PG/O₂-V, PG@A/O₂-H, PG@A/O₂-V, PG@B/O₂-H, and PG@B/O₂-V. In Figure 2, δ_0 represents the distance between the centroids of the molecule and the PG lattice. By varying δ_0 , the O₂ moved towards the PG plane and we obtained adsorption energy (E_{ads}) curves using the expression: $E_{ads} = E_{(PG+O_2)} - E_{PG} - E_{O_2}$, where E_{PG} , E_{O_2} , and $E_{(PG+O_2)}$ are the total energies for isolated PG, isolated O₂, and O₂ adsorbed on PG surface, respectively. For a more detailed description of the PG/O₂ adsorption mechanism, the case of higher adsorption energy

is further investigated through its electronic properties. This case was identified through the adsorption energy curves. These curves were fitted using the Improved Lennard-Jones (ILJ) equation [45].

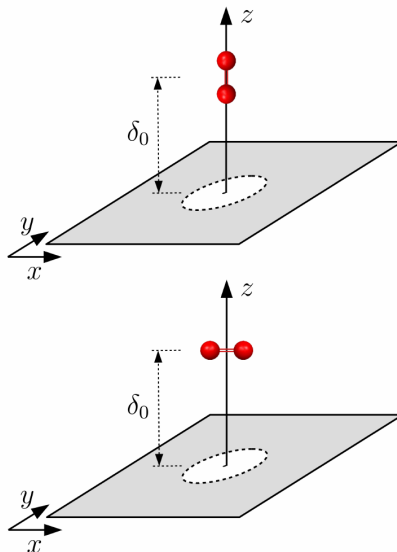


Figure 2: Schematic representation of the computational approach (initial system configurations) used here to obtain the adsorption energy curves for the O₂ interaction with all the PG lattices presented in Figure 1. The O₂ molecule is initially positioned 7 Å above the PG plane.

3. Results

We begin our discussions by presenting the adsorption energy curves that were obtained using the protocol discussed above. Figure 3 displays these curves and their related ILJ fitting [45]. In this figure, one can note that the interplay between the adsorption energy and the distance between O₂ and PG yields typical potential energy curves. The PG/O₂-H, PG/O₂-V, PG@B/O₂-H, and PG@B/O₂-V showed a physisorption mechanism since their curves do not present a clearly defined potential well. In these systems, the electronic properties of the adsorbent are slightly changed in the presence of an adsorbate (as discussed later). The obtained adsorption energies (ϵ parameter in reference [45]) and equilibrium distances (r_m) are presented in Table 1. These values for PG/O₂-H, PG/O₂-V, PG@B/O₂-H, and PG@B/O₂-V cases are similar to the ones obtained in other theoretical studies in which the adsorption of an oxygen molecule on pristine boron-nitride and graphene membranes were considered [46, 47]. A different adsorption mechanism is obtained for PG lattices endowed with a sp^3 -type vacancy. In Figure 3, one can note that the PG@A/O₂-H and PG@A/O₂-V cases present higher reactivity (or higher adsorption energies) than the other cases. The adsorption energy for the PG@A/O₂-H case is, at least, twice higher than all the other cases. Particularly, the adsorption process in PG@A/O₂-H system denotes a chemisorption mechanism, and the electronic properties of the PG are affected by its interaction with the O₂ molecule, as it will be discussed later. In contrast with the PG and PG@B cases, the PG@A/O₂-

The PG@A/O₂-V curves present a potential well. The vertical orientation of the O₂ molecule, regarding the PG plane, leads the two oxygen atoms to interact almost in the same fashion with the PG@A sheet. This trend is not observed in the PG@A/O₂-V case in which only one of the oxygen atoms is positioned close to the PG@A surface. Moreover, in the PG@A lattice, the atoms within the defective region are closer to each other than in the PG@B one. This feature is due to a tendency of the carbon atoms in forming new bonds in the vicinity of the vacancy, which reduces the area of the defective region and increases the electrostatic potential.

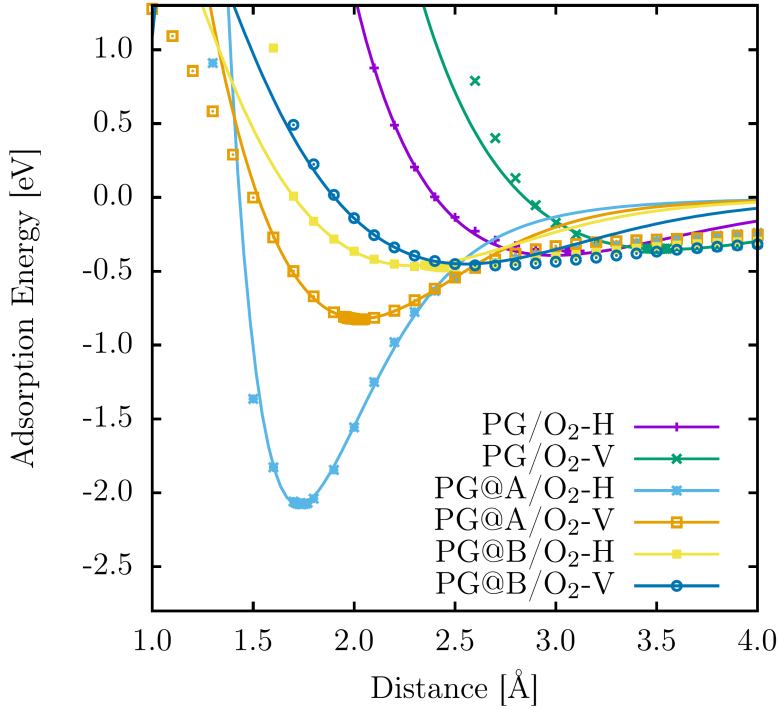


Figure 3: Adsorption energy curves for all the PG/O₂ complexes studied here. The curves were fitted using the ILJ equation [45]. The initial configurations are illustrated in Figure 2.

System	ϵ [eV]	r_m [Å]
PG/O ₂ -H	0.39	2.99
PG/O ₂ -V	0.35	3.55
PG@A/O ₂ -H	2.08	1.72
PG@A/O ₂ -V	0.82	2.03
PG@B/O ₂ -H	0.46	2.29
PG@B/O ₂ -V	-0.53	2.55

Table 1

Calculated adsorption energies ϵ and equilibrium distances r_m from the curve fitting presented in Figure 3, which was performed through the ILJ equation [45].

Now, we analyze the recovering time (τ) [48] — that corresponds to the transient time in which the molecule adsorption takes place — for the systems with better adsorption performances (PG@A/O₂-H e PG@A/O₂-V). The recovering time is calculated as $\tau = 1\nu \times \exp(-E_{ads}/k_B T)$, where ν is the molecule oscillation frequency ($10^{12} s^{-1}$)

[49]), k_B is the Boltzmann constant, and T the temperature (298 K). In Figure 4, the recovering time values for PG@A/O₂-H and PG@A/O₂-V adsorption energy curves are presented in the color palette. In this way, one can note that the recovering time varies from 0.5 ps up to 2.5 ps. For the lowest absorption energy (PG@A/O₂-H case) $\tau = 2.31$ ps whereas for the PG@A/O₂-V one, the highest recovering time is about 1.5 ps. It is worthwhile to stress that the transient times obtained for the O₂ adsorption in the PG@A lattice are large enough to realize the interaction between them, which changes the electronic properties of the PG (as discussed below), before the molecule diffusion.

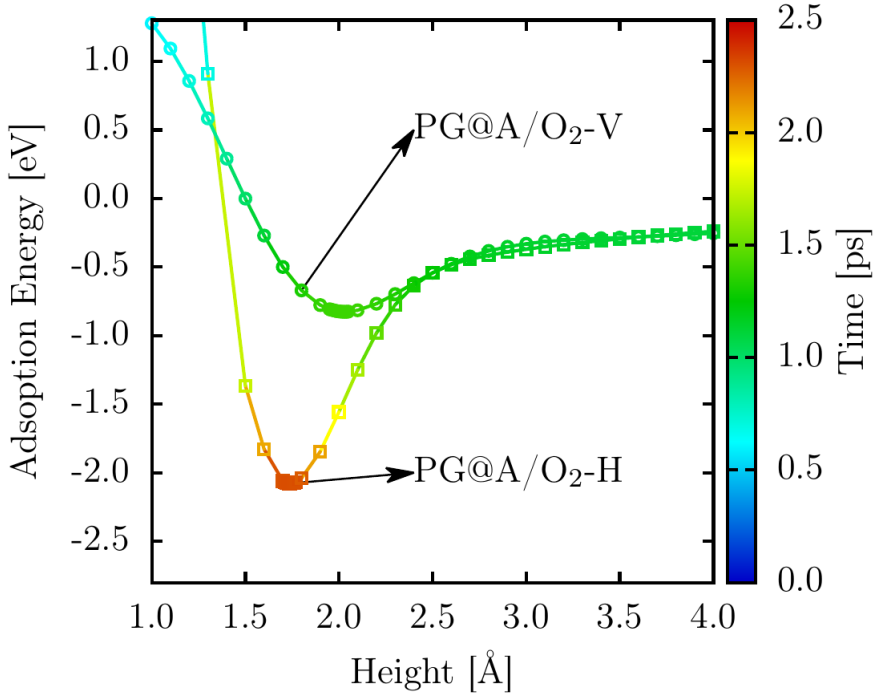


Figure 4: Recovering time values for PG@A/O₂-H and PG@A/O₂-V adsorption energy curves, depicted in Figure 3. The recovering time values are presented in the color palette.

The electronic band structures for the systems investigated here are presented in Figure 5. The left-most panel illustrates that the non-defective PG presents a quasi-direct bandgap of about 2.35 eV, which is in good agreement with the values reported in the references [19, 23, 30]. As expected, the inclusion of a single-atom vacancy leads to the appearance of energy levels within the bandgap. Similar band structure signatures for the PG@A and PG@B cases were reported in other DFT-based studies [30]. Upon adsorption, the valence and conduction bands of non-defective PG suffer an energy shifting (about -1.1 eV) for the PG/O₂-H and PG/O₂-V cases, preserving the initial PG bandgap value, and a flat midgap level (the O₂ energy level) appears nearby the Fermi level. These small changes in the bandgap configuration for the non-defective PG/O₂-H and PG/O₂-V systems, and their related low values of absorption energy, denote that this kind of PG lattice is not a useful nanostructure when it comes to gas sensing applications. This trend was also reported for the graphene case [46, 47]. The four right-most panels (PG@A/O₂-H, PG@A/O₂-V, PG@B/O₂-

H, PG@B/O₂-V) show that electronic band structure of defective PG lattices upon O₂ adsorption are substantially impacted. As discussed above, these cases have presented higher adsorption energies. Their bandgap configurations show the following common trend: upon adsorption, the bandgap value is slightly decreased and some flat midgap levels are formed. The PG@B/O₂ band structures are insensitive to the O₂ orientation regarding the PG plane whereas the PG@A/O₂ ones show changes in their configuration (i.e., PG@A lattice present a degree of selectivity).

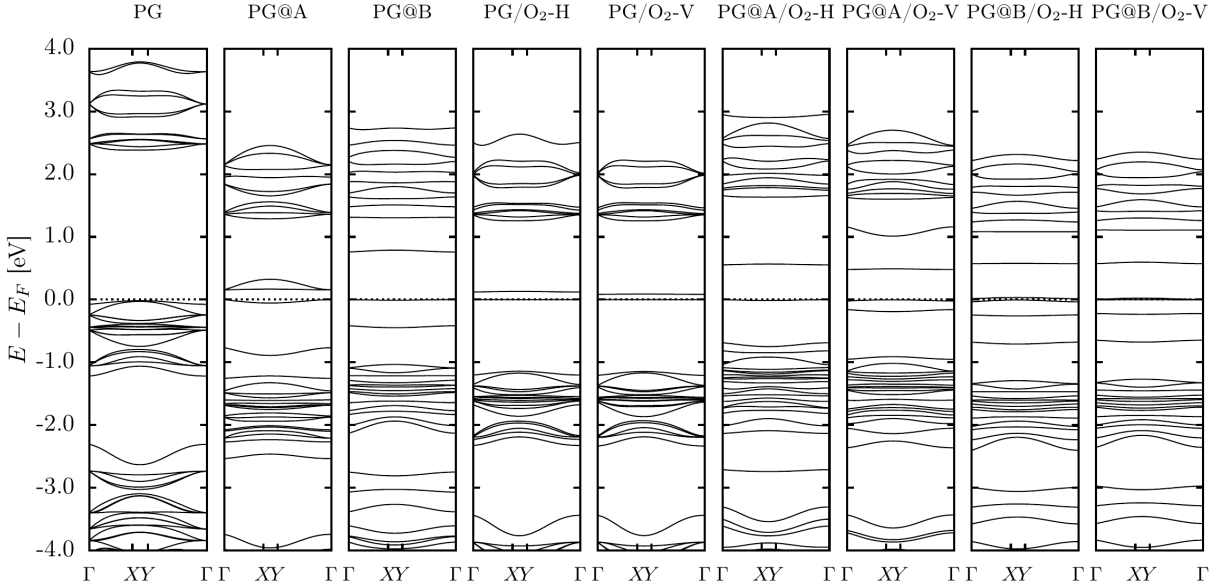


Figure 5: Electronic band structures for the systems investigated.

Finally, we analyze the electrostatic potential over the structure as well as the Highest Occupied Molecular Orbital (HOMO) and Lowest Unoccupied Molecular Orbital (LUMO) configurations only for the of better adsorption performance (PG@A/O₂). The top and bottom panels of Figure 6 illustrate, respectively, the HOMO and LUMO orbitals and the electronic potential. The PG@A/O₂-H shows the better reactivity among all the systems, once the O₂ molecule has a considerable degree of electronegativity while the PG@A lattice presents an excess of non-bonding electrons in the vicinity of the vacancy (*sp*³-like single-atom vacancy). This feature is illustrated by the electrostatic potential results, as shown in the bottom panels of Figure 6. The HOMO (green spots) and LUMO (pink spots) changed their localization upon the O₂ adsorption, as can be seen in the top panels of Figure 6. Notably, in the PG@A/O₂-H, part of the O₂ HOMO/LUMO orbital is delocalized on the PG surface. In this delocalization pattern, overlapping between the O₂ and PG@A orbitals takes place, which considerably enhances the interaction between. This orbitals overlapping is the main responsible in promoting the higher adsorption energy values and, consequently, the higher recovering time and changes in the electronic band structure discussed above (Figures 4 and 5, respectively). It is worthwhile that in the PG@B cases (*sp*²-like single-atom vacancy) the bond reconstructions (see Figure 1) substantially

diminishes the number of non-bonding electrons in the vicinity of the vacancy. Due to this reason, the PG@B cases presented lower adsorption energies when contrasted to the PG@A ones.

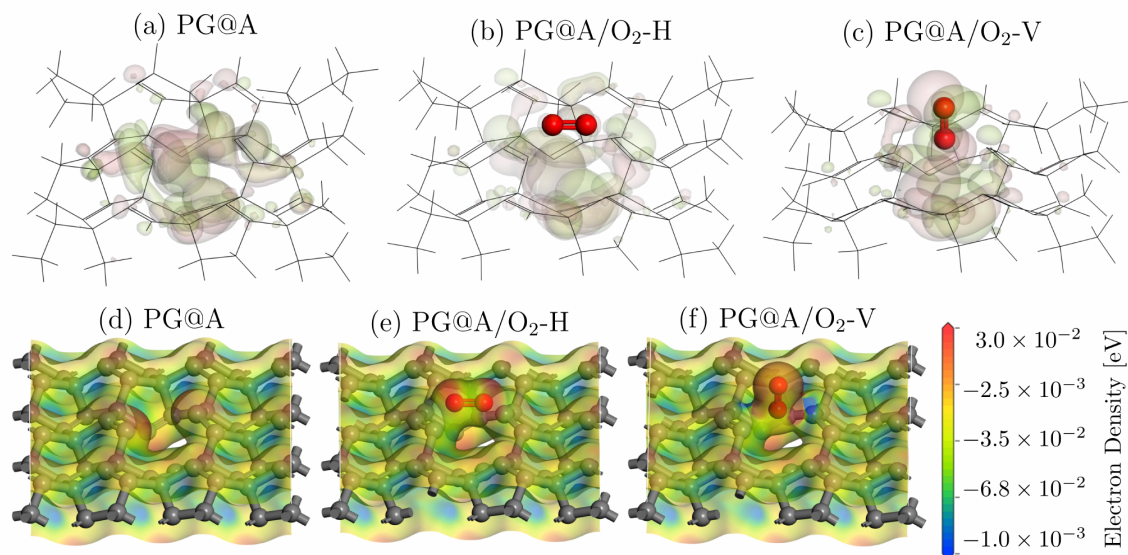


Figure 6: (top panels) Electrostatic potential over the structure and (bottom panels) the Highest Occupied Molecular Orbital (HOMO) and Lowest Unoccupied Molecular Orbital (LUMO) configurations for the case of higher adsorption energy (PG@A/O₂). In the color scheme for the top panels, the HOMO and LUMO orbitals are represented by the green and pink spots, respectively.

4. Conclusions

In summary, we carried out DFT calculations to investigate the O₂ adsorption mechanism on the surface of PG lattices endowed of single-atom vacancies. Our results have revealed that the relationship between the adsorption energy and the distance between O₂ and PG yields typical potential energy curves. The PG/O₂-H, PG/O₂-V, PG@B/O₂-H, and PG@B/O₂-V showed a physisorption mechanism. On the other hand, the PG@A/O₂-H e PG@A/O₂-V cases present higher reactivity. The adsorption energy for the PG@A/O₂-H case is, at least, twice higher than all the other cases. Particularly, the adsorption process in PG@A/O₂-H system stands for a chemisorption mechanism.

The recovering time values for PG@A/O₂-H and PG@A/O₂-V adsorption energy curves varied from 0.5 ps up to 2.5 ps. For the lowest absorption energy (PG@A/O₂-H case) $\tau = 2.31$ ps whereas for the PG@A/O₂-V one, the highest recovering time is about 1.5 ps. These transient times were large enough to realize the interaction between O₂ and PG@A and they have allowed changes in the electronic properties of the PG@A lattice. The electronic band structure of defective PG lattices upon O₂ adsorption is substantially impacted. Their bandgap configurations show the following common trend: upon adsorption, the bandgap value is slightly decreased and some flat midgap levels

are formed. The PG@B/O₂ band structures are insensitive to the O₂ orientation regarding the PG plane whereas the PG@A/O₂ ones show changes in their configuration, by presenting a degree of selectivity.

In the PG@A/O₂-H, part of the O₂ HOMO/LUMO orbital is delocalized on the PG surface and overlapping between the O₂ and PG@A orbitals is observed, which considerably enhances the interaction between. This overlapping trend is the main responsible in promoting the higher adsorption energy values and, consequently, the higher recovering time and changes in the electronic band structure for the PG@A/O₂-H case.

Acknowledgements

The authors gratefully acknowledge the financial support from Brazilian Research Councils CNPq, CAPES, and FAPDF and CENAPAD-SP for providing the computational facilities. L.A.R.J. gratefully acknowledges, respectively, the financial support from FAP-DF and CNPq grants 00193.0000248/2019-32 and 302236/2018-0.

References

- [1] Daniel S Tyson, Jason Bialecki, and Felix N Castellano. Ruthenium (ii) complex with a notably longexcited state lifetime. *Chemical Communications*, (23):2355–2356, 2000.
- [2] Gongming Wang, Yichuan Ling, and Yat Li. Oxygen-deficient metal oxide nanostructures for photoelectrochemical water oxidation and other applications. *Nanoscale*, 4(21):6682–6691, 2012.
- [3] Marc-Antoine Stoeckel, Marco Gobbi, Sara Bonacchi, Fabiola Liscio, Laura Ferlauto, Emanuele Orgiu, and Paolo Samorì. Reversible, fast, and wide-range oxygen sensor based on nanostructured organometal halide perovskite. *Advanced Materials*, 29(38):1702469, 2017.
- [4] O Leenaerts, B Partoens, and FM Peeters. Adsorption of h 2 o, n h 3, co, n o 2, and no on graphene: A first-principles study. *Physical Review B*, 77(12):125416, 2008.
- [5] Fredrik Schedin, Andrei Konstantinovich Geim, Sergei Vladimirovich Morozov, EW Hill, Peter Blake, MI Katsnelson, and Kostya Sergeevich Novoselov. Detection of individual gas molecules adsorbed on graphene. *Nature materials*, 6(9):652–655, 2007.
- [6] Wei Hu, Nan Xia, Xiaojun Wu, Zhenyu Li, and Jinlong Yang. Silicene as a highly sensitive molecule sensor for nh 3, no and no 2. *Physical Chemistry Chemical Physics*, 16(15):6957–6962, 2014.
- [7] Wenjing Yuan, Anran Liu, Liang Huang, Chun Li, and Gaoquan Shi. High-performance no2 sensors based on chemically modified graphene. *Advanced Materials*, 25(5):766–771, 2013.
- [8] Lu Bai and Zhen Zhou. Computational study of b-or n-doped single-walled carbon nanotubes as nh3 and no2 sensors. *Carbon*, 45(10):2105–2110, 2007.
- [9] yacheslav O. Khavrus, Hartmut Vinzelberg, Joachim Schumann, Albrecht Leonhardt, Steffen Oswald, and Bernd BÄijchner. On the potential of long carbon nanotube forest for sensing gases and vapors. *Physica E: Low-dimensional Systems and Nanostructures*, 43(6):1199 – 1207, 2011.
- [10] Hubert Valencia, AdriÃã Gil, and Gilles Frapper. Trends in the adsorption of 3d transition metal atoms onto graphene and nanotube surfaces: A dft study and molecular orbital analysis. *The Journal of Physical Chemistry C*, 114(33):14141–14153, 2010.
- [11] Xianping Chen, Cell KY Wong, Cadmus A Yuan, and Guoqi Zhang. Nanowire-based gas sensors. *Sensors and Actuators B: Chemical*, 177:178–195, 2013.

- [12] Zhen Zhu and David Tománek. Semiconducting layered blue phosphorus: a computational study. *Physical review letters*, 112(17):176802, 2014.
- [13] Rui-Shen Meng, Miao Cai, Jun-Ke Jiang, Qiu-Hua Liang, Xiang Sun, Qun Yang, Chun-Jian Tan, and Xian-Ping Chen. First principles investigation of small molecules adsorption on antimonene. *IEEE Electron Device Letters*, 38(1):134–137, 2016.
- [14] Byungjin Cho, Myung Gwan Hahm, Minseok Choi, Jongwon Yoon, Ah Ra Kim, Young-Joo Lee, Sung-Gyu Park, Jung-Dae Kwon, Chang Su Kim, Myungkwon Song, et al. Charge-transfer-based gas sensing using atomic-layer mos 2. *Scientific reports*, 5:8052, 2015.
- [15] Jian Zhen Ou, Wanyin Ge, Benjamin Carey, Torben Daeneke, Asaf Rotbart, Wei Shan, Yichao Wang, Zhengqian Fu, Adam F Chrimes, Wojtek Wlodarski, et al. Physisorption-based charge transfer in two-dimensional sns2 for selective and reversible no2 gas sensing. *ACS nano*, 9(10):10313–10323, 2015.
- [16] P Blake, EW Hill, AH Castro Neto, KS Novoselov, D Jiang, R Yang, TJ Booth, and AK Geim. Making graphene visible. *Applied physics letters*, 91(6):063124, 2007.
- [17] Rahul Raveendran Nair, Peter Blake, Alexander N Grigorenko, Konstantin S Novoselov, Tim J Booth, Tobias Stauber, Nuno MR Peres, and Andre K Geim. Fine structure constant defines visual transparency of graphene. *Science*, 320(5881):1308–1308, 2008.
- [18] AH Castro Neto, Francisco Guinea, Nuno MR Peres, Kostya S Novoselov, and Andre K Geim. The electronic properties of graphene. *Reviews of modern physics*, 81(1):109, 2009.
- [19] Zhang Shunhong, Zhou Jian, Wang Qian, Chen Xiaoshuang, Kawazoe Yoshiyuki, and Jena Puru. Penta-graphene: A new carbon allotrope. *Radio electronics. Nanosystems. Information Technology.*, 7(2), 2015.
- [20] Christopher P. Ewels, Xavier Rocquefelte, Harold W. Kroto, Mark J. Rayson, Patrick R. Briddon, and Malcolm I. Heggie. Predicting experimentally stable allotropes: Instability of penta-graphene. *Proceedings of the National Academy of Sciences*, 112(51):15609–15612, 2015.
- [21] EM Stuve and RJ Madix. Use of the π - σ parameter for characterization of rehybridization upon adsorption on metal surfaces. *The Journal of Physical Chemistry*, 89(15):3183–3185, 1985.
- [22] FL Coffman, R Cao, PA Pianetta, S Kapoor, M Kelly, and LJ Terminello. Near-edge x-ray absorption of carbon materials for determining bond hybridization in mixed sp²/sp³ bonded materials. *Applied Physics Letters*, 69(4):568–570, 1996.
- [23] Hongbo Qin, Chuang Feng, Xinghe Luan, and Daoguo Yang. First-principles investigation of adsorption behaviors of small molecules on penta-graphene. *Nanoscale research letters*, 13(1):1–7, 2018.
- [24] Dachang Chen, Xiaoxing Zhang, Ju Tang, Hao Cui, Zhenwei Chen, and Yi Li. Different doping of penta-graphene as adsorbent and gas sensing material for scavenging and detecting sf6 decomposed species. *Sustainable Materials and Technologies*, 21:e00100, 2019.
- [25] Meng-Qi Cheng, Qing Chen, Ke Yang, Wei-Qing Huang, Wang-Yu Hu, and Gui-Fang Huang. Penta-graphene as a potential gas sensor for no x detection. *Nanoscale Research Letters*, 14(1):306, 2019.
- [26] Lin Li, Kaixuan Jin, Chunyan Du, and Xiaojie Liu. The effect of oxidation on the electronic properties of penta-graphene: first-principles calculation. *RSC advances*, 9(15):8253–8261, 2019.
- [27] Aaditya Manjanath, Chao-Ping Hsu, and Yoshiyuki Kawazoe. Tuning the electronic and magnetic properties of pentagraphene through the c1 vacancy. *2D Materials*, 2020.
- [28] Tran Yen Mi, Dang Minh Triet, and Nguyen Thanh Tien. Adsorption of gas molecules on penta-graphene nanoribbon and its implication for nanoscale gas sensor. *Physics Open*, 2:100014, 2020.
- [29] C. Feng, X. Luan, P. Zhang, J. Xiao, D. Yang, and H. Qin. A first-principle study of the adsorption behavior of no gas molecules on pristine and al-doped penta-graphene. In *2017 18th International Conference on Electronic Packaging Technology (ICEPT)*, pages 1138–1142, 2017.
- [30] John Isaac G. Enriquez and Al Rey C. Villagracia. Hydrogen adsorption on pristine, defected, and 3d-block transition metal-doped penta-

- graphene. *International Journal of Hydrogen Energy*, 41(28):12157 – 12166, 2016.
- [31] Landong Li, Junqing Yan, Tuo Wang, Zhi-Jian Zhao, Jian Zhang, Jinlong Gong, and Naijia Guan. Sub-10 nm rutile titanium dioxide nanoparticles for efficient visible-light-driven photocatalytic hydrogen production. *Nature communications*, 6(1):1–10, 2015.
- [32] Jaison Jeevanandam, Ahmed Barhoum, Yen S Chan, Alain Dufresne, and Michael K Danquah. Review on nanoparticles and nanostructured materials: history, sources, toxicity and regulations. *Beilstein journal of nanotechnology*, 9(1):1050–1074, 2018.
- [33] Imali A Mudunkotuwa and Vicki H Grassian. The devil is in the details (or the surface): impact of surface structure and surface energetics on understanding the behavior of nanomaterials in the environment. *Journal of Environmental Monitoring*, 13(5):1135–1144, 2011.
- [34] B. Delley. An all-electron numerical method for solving the local density functional for polyatomic molecules. *The Journal of Chemical Physics*, 92(1):508–517, 1990.
- [35] B. Delley. From molecules to solids with the dmol3 approach. *The Journal of Chemical Physics*, 113(18):7756–7764, 2000.
- [36] Jan Andzelm, Christoph K ulmel, and Andreas Klamt. Incorporation of solvent effects into density functional calculations of molecular energies and geometries. *The Journal of Chemical Physics*, 103(21):9312–9320, 1995.
- [37] John P Perdew and Yue Wang. Accurate and simple analytic representation of the electron-gas correlation energy. *Physical review B*, 45(23):13244, 1992.
- [38] Walter Kohn and Lu Jeu Sham. Self-consistent equations including exchange and correlation effects. *Physical review*, 140(4A):A1133, 1965.
- [39] B. Delley. Hardness conserving semilocal pseudopotentials. *Phys. Rev. B*, 66:155125, Oct 2002.
- [40] Hendrik J. Monkhorst and James D. Pack. Special points for brillouin-zone integrations. *Phys. Rev. B*, 13:5188–5192, Jun 1976.
- [41] Kleuton Antunes Lopes Lima, Wiliam Ferreira da Cunha, F bio Ferreira Monteiro, Marcelo Lopes Pereira Jr, and Luiz Antonio Ribeiro Jr. Adsorption of carbon dioxide and ammonia in transition metal-doped boron nitride nanotubes. *Journal of Molecular Modeling*, 25, 2019.
- [42] Edson Nunes Costa Paura, Wiliam F. da Cunha, Pedro H. de Oliveira Neto, Geraldo M. e Silva, Joao B. L. Martins, and Ricardo Gargano. Vibrational and electronic structure analysis of a carbon dioxide interaction with functionalized single-walled carbon nanotubes. *The Journal of Physical Chemistry A*, 117(13):2854–2861, 2013. PMID: 23425025.
- [43] Edson N. C. Paura, Wiliam F. da Cunha, Jo o Batista Lopes Martins, Geraldo Magela e Silva, Luiz F. Roncaratti, and Ricardo Gargano. Carbon dioxide adsorption on doped boron nitride nanotubes. *RSC Adv.*, 4:28249–28258, 2014.
- [44] Igo T. Lima, Ricardo Gargano, Silvete Guerini, and Edson N. C. Paura. A theoretical study of adsorbed non-metallic atoms on magnesium chloride monolayers. *New J. Chem.*, 43:7778–7783, 2019.
- [45] Fernando Pirani, Simona Brizi, Luiz F. Roncaratti, Piergiorgio Casavecchia, David Cappelletti, and Franco Vecchiocattivi. Beyond the lennard-jones model: a simple and accurate potential function probed by high resolution scattering data useful for molecular dynamics simulations. *Phys. Chem. Chem. Phys.*, 10:5489–5503, 2008.
- [46] H. J. Yan, B. Xu, S. Q. Shi, and C. Y. Ouyang. First-principles study of the oxygen adsorption and dissociation on graphene and nitrogen doped graphene for li-air batteries. *Journal of Applied Physics*, 112(10):104316, 2012.
- [47] Qiao Sun, Caixia Sun, Aijun Du, Shixue Dou, and Zhen Li. In-plane graphene/boron-nitride heterostructures as an efficient metal-free electrocatalyst for the oxygen reduction reaction. *Nanoscale*, 8:14084–14091, 2016.
- [48] Kriengkri Timsorn and Chatchawal Wongchoosuk. Adsorption of NO₂, HCN, HCHO and CO on pristine and amine functionalized boron nitride nanotubes by self-consistent charge density functional tight-binding method. *Materials Research Express*, 7(5):055005, may 2020.
- [49] Shu Peng, Kyeongjae Cho, Pengfei Qi, and Hongjie Dai. Ab initio study of cnt no₂ gas sensor. *Chemical Physics Letters*, 387(4):271 – 276, 2004.